

## Original Article

# Combined inhibition of FGFR4 and VEGFR signaling enhances efficacy in FGF19 driven hepatocellular carcinoma

Xuesong Zhao\*, Jaya Julie Joshi\*, Daniel Aird, Craig Karr, Kun Yu, Chialing Huang, Federico Colombo, Milena Virrankoski, Sudeep Prajapati, Anand Selvaraj

Department of Discovery, H3 Biomedicine Inc., Cambridge, MA 02139, USA. \*Equal contributors.

Received February 8, 2022; Accepted April 7, 2022; Epub June 15, 2022; Published June 30, 2022

**Abstract:** Hepatocellular carcinoma (HCC) is an aggressive liver malignancy that is difficult to treat with no approved biomarker based targeted therapies. FGF19-FGFR4 signaling blockade has been recently identified as a promising avenue for treatment of a subset of HCC patients. Using HCC relevant xenograft and PDX models, we show that Lenvatinib, an approved multi-kinase inhibitor, strongly enhanced the efficacy of FGFR4 inhibitor H3B-6527. This enhanced combination effect is not due to enhanced FGFR4 inhibition and it is likely due to cell non-autonomous VEGFR activity of Lenvatinib. This cell non-autonomous mode of action was further supported by strong *in vivo* combination efficacy with the mouse specific VEGFR2 antibody, DC101, which cannot cell-autonomously inhibit pathways in human xenografts. Mechanistic studies showed that the combination resulted in enhanced efficacy through increased anti-angiogenic and anti-tumorigenic activities. Overall, our results indicate that this combination can be a highly effective treatment option for FGF19 driven HCC patients, and provide preclinical validation of a combination that can be readily tested in the clinical setting.

**Keywords:** HCC, FGF19, FGFR4, VEGFR, H3B-6527, Lenvatinib

## Introduction

HCC is the most common primary liver malignancy and is a leading cause of cancer-related death worldwide with an increasing rate of incidence and mortality [1]. Due to its heterogeneity and aggressive nature, advanced HCC is a very difficult disease to treat and for many years Sorafenib was the only systemic treatment for advanced HCC [2]. Recent approvals of multi-kinase inhibitors and immune checkpoint inhibitors have provided much needed treatment options for HCC patients [3]. Apart from the immune checkpoint inhibitors, all of the approved systemic agents in HCC mediate their anticancer effect largely through the Vascular endothelial growth factor-Vascular endothelial growth factor receptor (VEGF-VEGFR) pathway demonstrating the importance of angiogenesis in HCC progression [4]. While these anti-angiogenic agents and immune checkpoint inhibitors offered some benefit to patients, the un-met medical need in advanced

HCC remains high [5]. Large-scale Next-Generation Sequencing (NGS) has shown mutations in the *TERT* promoter, *CTNNB1*, *TP53*, and *ARID1A*, and provided new avenues for potential therapies [6]. Apart from these mutations, these studies have also reported overexpression of several cancer driver genes including cyclin D1 (*CCND1*) and fibroblast growth factor 19 (FGF19) providing additional paths for new therapies [7]. Among these genomic and transcriptomic alterations, FGF19 alteration has generated a lot of interest due to its liver-specific physiology [8].

FGF19 is a gut-secreted endocrine hormone that controls bile acid synthesis in the liver through its activation of fibroblast growth factor receptor 4 (FGFR4) [8]. In genetically engineered mouse model (GEMM) studies, overexpression of FGF19 promoted liver tumorigenesis through the activation of FGFR4, and FGFR4 blockade prevented tumor formation [9]. This compelling evidence from patient samples and

mouse models prompted drug discovery efforts against FGFR4 resulting in the generation of multiple FGFR4 selective inhibitors including H3B-6527 [10, 11]. Consistent with the mouse genetic studies, these pharmacological agents prevented FGF19 induced tumorigenesis in cell line and patient-derived mouse xenografts [10-12]. Most importantly, early phase clinical trials translated the preclinical work and reported that 15-20% of FGF19 driven HCC patients responded to the FGFR4 selective inhibitor treatment [12]. While these studies validated FGFR4 as an HCC therapeutic target, the clinical benefit for this single-agent treatment remains limited potentially requiring combination approaches to improve the outcome. Given the central role of angiogenesis in HCC progression, we hypothesized that dual inhibition of FGFR4 and VEGFR pathways may disrupt tumorigenesis and angiogenesis, and provide deeper and broader anti-tumor activity for FGF19 driven cancers. Apart from its role in mediating the FGF19 driven tumorigenesis, FGFR4 also plays an important role in the development of resistance to antiangiogenic therapy [13], providing further rationale for testing this combination. Here we test this hypothesis using H3B-6527 as the FGFR4 inhibitor, Lenvatinib and VEGFR2 antibodies as VEGFR blockades in the preclinical models, and provide evidence that this combination can be a highly effective treatment option for FGF19 driven HCC patients.

### Materials and methods

#### *Preparation of Lenvatinib, H3B-6527, and DC101 for in vivo experiments*

Lenvatinib was formulated in distilled water. H3B-6527 was formulated in 0.5% methylcellulose (Sigma, CAS: 9004-67-5) and 0.2% Tween 80 (Sigma, Cat: P4780). DC101 (Bioxcell, BPO060) antibody stock solutions were diluted in saline to get 8 mg/mL before use.

#### *RNA-seq analysis*

Total RNA was extracted and purified from 50 to 100 mg tumor fragments using RNeasy reagent (Qiagen). mRNA libraries were prepared for sequencing using standard Illumina protocols. The sequencing reads were produced by the Illumina HiSeq 4000, and aligned with both human reference (GRCh37) and the mouse reference genomes (GRCm38) using

STAR [14]. The aligned BAM files were processed by the in-house xenotool to generate the high quality human BAM files and remove mouse reads. The transcripts abundance was calculated using Kallisto [15]. EdgeR v3.16.5 Bioconductor library [16] with trimmed mean of M values (TMM) normalization was used to generate the normalized and log2 transformed RNA-seq data in R v3.2.3 statistical environment (<http://www.r-project.org>). Non-protein coding transcripts and low expressed genes (genes with log2 (tpm) < 2 in all samples) were excluded. Low variation genes (genes with variation < 0.1 across all samples) were filtered out. 1818 genes with the most variation were selected to generate PCA plot. 9080 significantly differentially expressed genes (adjusted *p* value < 0.05) were reported. For gene differential expression and GSEA analysis, the genes were ranked by fold changes of the treatment comparing to vehicle. The GSEA pre-ranked gene list was used to obtain the enriched hallmark gene sets (v5.2 MSigDB) in each group [17, 18]. Hallmark gene sets with normalized *p*-value < 0.01 in at least one treatment group were reported. The RNAseq data have been deposited in the Gene Expression Omnibus (GEO) repository under accession number GSE198845.

#### *RT-qPCR assay for CYP7A1*

RNA was extracted from tumor fragments using Tri reagent (Ambion) and Omni Bead Ruptor. cDNA was synthesized using SuperScript Enzyme Mix (Thermo Fisher Scientific). RT-qPCR of CYP7A1 were measured using TaqMan Gene Expression kit on the ViiA7TM Real-Time PCR System (Thermo Fisher Scientific). RT-qPCR data were normalized by subtracting the 18S endogenous control Ct value from the CYP7A1 Ct value, then subtracting that value from the average vehicle control Ct value for that time point. Levels of CYP7A1 gene expression were determined by raising 2 to the delta delta Ct value.

#### *Cell culture, compound treatment, and viability assay*

Hep3B cells (purchased from American Type Culture Collection (ATCC), Address: 10801 University Boulevard, Manassas, VA 20110, USA) were maintained in Eagle's Minimum Essential Medium (ATCC, 30-2003) with 10% fetal bovine serum. The cells were cultured in a humidified

## Enhanced efficacy in HCC by combining FGFR4 and VEGFR inhibition

incubator at 37°C with 5% CO<sub>2</sub>. Compounds were dissolved in dimethyl sulfoxide (DMSO). Stock concentration is 10 mM. The final percentage of DMSO in testing media was 0.1%. Cells were harvested during the logarithmic growth phase and seeded into 96-well plates. The treatment was 72 h. The viability measurements were performed by adding 50 µL of CellTiter-Glo® Viability Assay reagent (Promega) to each well. Luminescence signals were measured on the Envision plate reader after shaking assay plates for 2 minutes. GI<sub>50</sub> (the concentration of test article at which cell growth is inhibited by 50% compared to vehicle treated cells) was calculated according to the publication from NCI [19]. Combination effects of *in vitro* viability were assessed using Chalice software (Horizon Discovery) comparing combination responses to their matched single-agent effects using the Loewe Additivity Model [20, 21]. Quantitative assessment was made by the Chalice synergy score.

### *In vivo antitumor activity in subcutaneous xenograft and PDX models*

The BALB/c nu/nu female mice approximately 8-weeks old, weighing 18-20 g were obtained from Jackson laboratory, Bar Harbor, ME. For the Hep3B xenografts, cells were harvested in exponential growth phase, and suspended in a 1:1 mixture of RPMI1640 medium containing 10% fetal bovine serum and Matrigel (Corning) at a final concentration of 5 × 10<sup>7</sup> cells/mL. 0.1 mL of the inoculum was injected subcutaneously into the right flank region of mice. Mice were randomized into treatment groups when the mean tumor volume (TV) reached approximately 120-200 mm<sup>3</sup>, 8 mice per group. Treatment with H3B-6527 or Lenvatinib or the combination was administered by oral gavage either at once daily (QD) or twice daily (BID) as indicated in the figures. DC101 was administered via intraperitoneal injection (ip) once every three days (Q3D). Tumors for RNA-seq studies were collected at 8 hour post the 4th dose at once daily (QD), 3 mice per group. The PDX efficacy studies were performed by Shanghai ChemPartner [22]. For these PDX studies, 6-8 week-old female Nu/Nu mice weighing 16-19 g were purchased from Beijing Vital River Laboratory Animal Technology Co. Ltd. (Beijing, China). The PDX studies were conducted using 8 animals per group.

Body weights were measured daily and tumor measurements were performed twice weekly. Mice with > 20% body weight loss or mice bearing tumors with the longest diameter > 2000 mm were euthanized to prevent any suffering according to IACUC guidelines defined by the H3 Biomedicine Animal Care and Use Program and study protocol. The TV in mm<sup>3</sup> was calculated according to the following formula: TV = length × width<sup>2</sup> × 0.5 length: largest diameter of tumor (mm) width: diameter perpendicular to length (mm). The Tumor Growth Inhibition% (TGI) was calculated according to the following formula: Tumor Growth Inhibition% (TGI) = [((Average control TV day X - TV day 0) - (Average treatment TV day X - TV day 0))/(Average control TV day X - TV day 0)] × 100, where Day X is any day of treatment. The anti-tumor effects of the treatment were defined as follows: Progressive disease (PD): 3 consecutive measurements > 120% of starting volume or 3 consecutive increasing measurements from best response, Stable disease (SD): 3 consecutive measurements > 50% and < 120% of starting volume, Partial regression (PR): 3 consecutive measurements < 50% of starting volume, Complete regression (CR): 3 consecutive measurements < 30 mm<sup>3</sup>.

## Results

### *Lenvatinib enhances H3B-6527 efficacy in vivo in the FGF19 positive HCC Hep3B xenograft model*

H3B-6527, a selective and covalent FGFR4 inhibitor, is efficacious as a single agent in the FGF19 positive HCC models [10]. Liver tumors are enriched with vasculature and are highly dependent on the VEGFR pathway [23]. To test whether combined inhibition of FGFR4 and VEGFR provide enhanced antitumor activity *in vivo*, we performed a combination experiment with H3B-6527 and Lenvatinib, an approved VEGFR inhibitor, in the FGF19 positive HCC Hep3B cell line xenograft model. We had previously shown that H3B-6527 single agent at a dose of 300 mg/kg twice daily is sufficient to cause tumor regression in this FGFR4 dependent model [10]. To examine the combination effect, we reduced the dose level of H3B-6527 to 300 mg/kg once daily and combined this with Lenvatinib, at dose levels of 3 or 10 mg/kg once daily, both by oral administration. Supporting the hypothesis, this combination

## Enhanced efficacy in HCC by combining FGFR4 and VEGFR inhibition

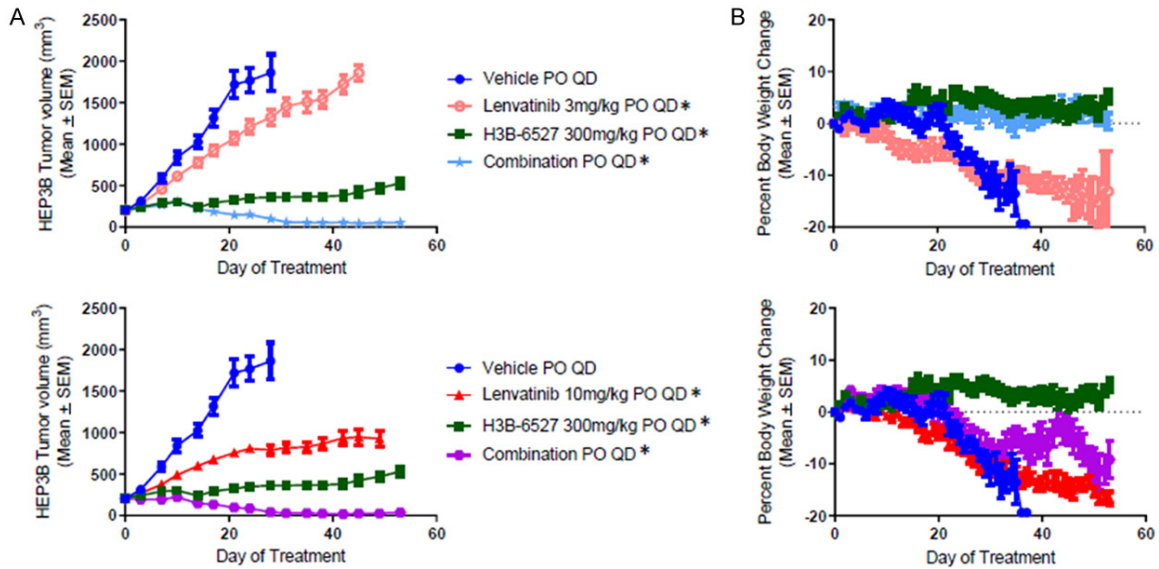


**Figure 1.** Antitumor effects following H3B-6527 and Lenvatinib as single agents or in combination in Hep3B HCC cell line xenografts grown in female nude mice. (A) Tumor volume and (B) Body weight measurements following oral dosing of H3B-6527 and Lenvatinib at indicated doses and schedule. QD, Once daily dose; PO, Per os (oral dosing). Data represent the mean  $\pm$  SEM (N = 8). For TV comparisons, \*P < 0.05 for all treatment groups compared to vehicle control on day 21 (Two way ANOVA with Holm Sidak's post hoc correction); \*P < 0.05 for the combination treatment groups compared to single treatment groups on day 21 (Two way ANOVA with Holm Sidak's post hoc correction). All tumor volume and body weight curves are from the same study.

resulted in robust tumor regression (TGI of 104% and 107% for the Lenvatinib 3 and 10 mg/kg combination treatment groups on day 21, respectively; **Figure 1A**), whereas the H3B-6527 or Lenvatinib single arms led only to tumor stasis or partial growth inhibition (TGI of 43%, 64% and 92% for the Lenvatinib 3 and 10 mg/kg, and H3B-6527 single treatment groups on day 21, respectively; **Figure 1A**). Importantly, the combination treatment is well tolerated in mice, and the body weight loss observed in the vehicle and the Lenvatinib single agent treatment groups due to Hep3B xenografts-induced cachexia [24], was prevented by the H3B-6527 single or combination treatment with Lenvatinib (**Figure 1B**).

*Enhanced efficacy mediated by Lenvatinib in vivo is not a result of enhanced FGFR4 inhibition*

Lenvatinib antitumor effects are largely mediated by VEGFRs, however it is known to also inhibit FGFRs including FGFR4 [5, 25]. To determine whether the enhanced efficacy observed above was due to deeper inhibition of FGFR4 instead of combined effect of FGFR4 and VEGFR, we evaluated the FGFR4 downstream

signaling. Plasma and tumor samples were collected at designated time points after a single dose of H3B-6527 at 300 mg/kg, Lenvatinib at 10 mg/kg and a combination of those two agents in Hep3B cell line xenografts. First, H3B-6527 and Lenvatinib plasma and tumor measurements showed that the two agents did not affect each other's exposure levels as the levels were comparable to single agent treatment groups (**Figure 2A**). Next, we measured CYP7A1 in tumor tissue, a *bona fide* FGFR4 downstream effector and the major rate limiting enzyme in the bile acid synthesis pathway. Consistent with the historical data, H3B-6527 single agent treatment raised CYP7A1 levels which peaked at 4 hours and then decreased with time (**Figure 2B**) [10]. In contrast, Lenvatinib single agent at 10 mg/kg did not elevate CYP7A1 expression appreciably suggesting that FGFR4 is not inhibited by Lenvatinib at this dose level. Importantly, the CYP7A1 levels in the combination group resembled the single agent H3B-6527 group suggesting the enhanced combination efficacy is not due to deeper FGFR4 inhibition (**Figure 2B**). To extend the single dose study, we also conducted a 4-day repeat-dose study and found only a very modest transient increase of tumor CYP7A1 expres-

## Enhanced efficacy in HCC by combining FGFR4 and VEGFR inhibition

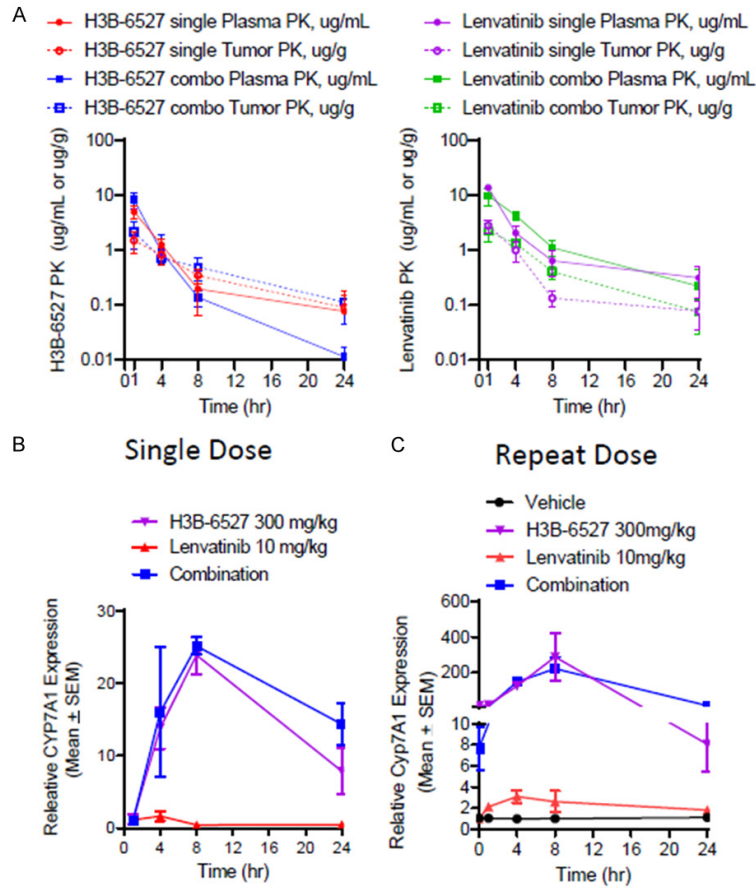


**Figure 2.** FGFR4 inhibition as measured by CYP7A1 following H3B-6527 and Lenvatinib as single agents or in combination in Hep3B *in vivo*. **A.** Tumor and plasma H3B-6527 and Lenvatinib concentrations at indicated time points after a single dose of H3B-6527 at 300 mg/kg or Lenvatinib at 10 mg/kg as single agents or together as combination. **B.** Relative expression levels of CYP7A1 at indicated time points after a single dose of compounds administered orally. **C.** Relative expression levels of CYP7A1 at indicated time points after a repeat dose of compounds administered orally. Data represent the mean  $\pm$  SEM (N = 3). No significance between H3B-6527 and combination group at any time point (Two way ANOVA with Sidak's post hoc correction).

sion in the Lenvatinib single agent group. In contrast, tumor CYP7A1 levels in both H3B-6527 single and combination groups were about ~100 fold higher at the peak time point and remained elevated across each time point (**Figure 2C**). Taken together, these data suggest that Lenvatinib mediated enhancement of H3B-6527 efficacy in Hep3B does not occur through enhanced inhibition of FGFR4.

*Enhanced efficacy mediated by Lenvatinib is likely cell non-autonomous*

H3B-6527 is known to reduce tumorigenesis largely through cell autonomous effects as evi-

dent from the strong *in vitro* viability effects, however Lenvatinib effects can be mediated through both cell autonomous and non-autonomous manner [25]. To test whether the enhanced combination efficacy observed in Hep3B *in vivo* is cell autonomously driven, we conducted an *in vitro* study in Hep3B and measured cell growth via an ATP-based cell viability assay. First, single agent H3B-6527 or Lenvatinib, tested in a dose response, resulted in GI<sub>50</sub> values (concentration of inhibitor that led to a 50% reduction in viability) of 8.5 and 446 nmol/L, respectively, in the Hep3B cells (**Figure 3A**). This strong growth inhibition by H3B-6527 and weak growth inhibition by Lenvatinib *in vitro* is not surprising as these models are highly FGFR4 dependent and H3B-6527 is a much more potent FGFR4 inhibitor than Lenvatinib. Next, we conducted a combination study of H3B-6527 and Lenvatinib in a dose response matrix, and found the combination led to very weak additivity but no synergistic growth effects *in vitro* in Hep3B (**Figure 3B** and **3C**). These data support the possibility that the *in vivo* enhancement of H3B-6527 efficacy by Lenvatinib is likely due to cell

non-autonomous mode of action and likely through the VEGFR mediated tumor microenvironment effects. To directly and selectively test the microenvironment effects, we applied DC101 [26, 27], a mouse-specific VEGFR2 antibody in a combination *in vivo* study in the Hep3B *in vivo* xenograft setting. H3B-6527 at 300 mg/kg once daily as single agent resulted in tumor stasis in this study and DC101 at 1600 ug single agent group showed partial tumor growth inhibition (TGI of 85.9% and 49.5% for the DC101 and H3B-6527 single treatment groups on day 18, respectively; **Figure 3D**). The dose level of DC101 at 1600 ug was chosen based on literature evidence [28] and maxi-

## Enhanced efficacy in HCC by combining FGFR4 and VEGFR inhibition

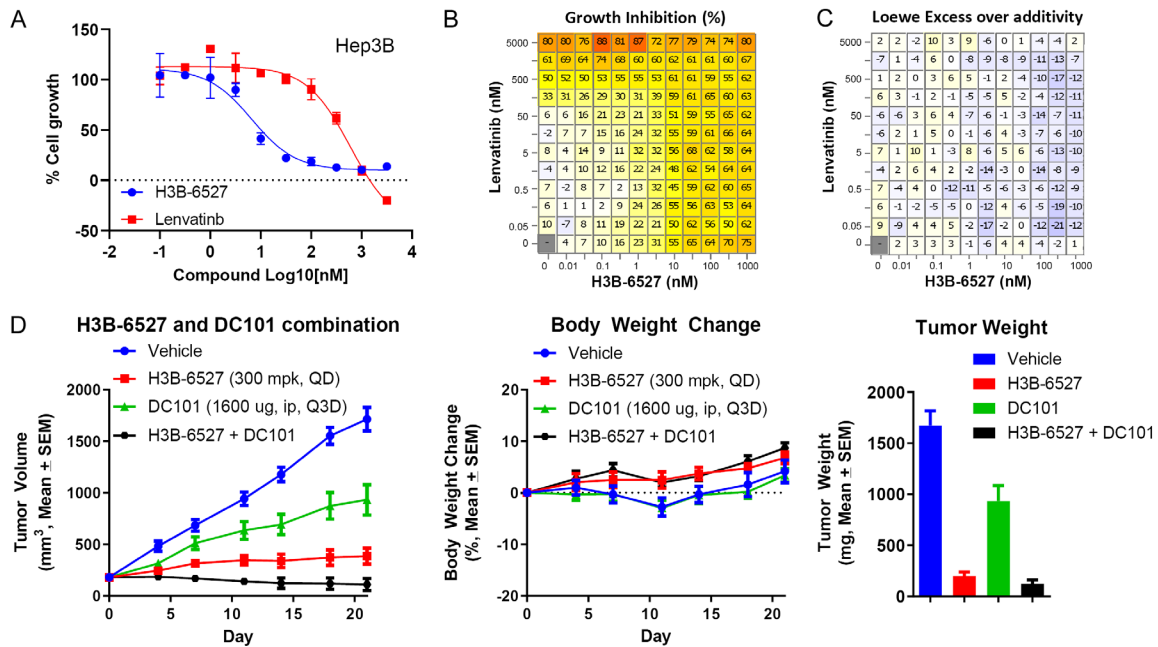


**Figure 3.** H3B-6527 and Lenvatinib effects in the HCC cell line Hep3B *in vitro*. A. Representative H3B-6527 and Lenvatinib dose response curves for ATP based cell viability assay. B. Representative H3B-6527 and Lenvatinib dose response matrix for ATP based cell viability assay. C. Chalice software was used to calculate excess inhibition over Loewe additivity for H3B-6527 and Lenvatinib dose combination. D. Antitumor effects following H3B-6527 and anti-VEGFR combination treatment in Hep3B HCC cell line xenografts grown in female nude mice. Tumor volume and Body weight measurements following H3B-6527 and DC101 treatment at indicated doses and schedule. Tumor weight measurements on day 21. H3B-6527 was administered by oral gavage, once daily dose (QD). DC101 was administered via intraperitoneal injection (ip) once every three days (Q3D). Data represent the mean  $\pm$  SEM (N = 8). For TV comparisons,  $P < 0.05$  for all treatment groups when compared to vehicle control on day 21 (Two way ANOVA with Holm Sidak's post hoc correction);  $P < 0.05$  for the combination treatment group compared to single treatment groups on day 21 (Two way ANOVA with Holm Sidak's post hoc correction). For Tumor weight comparisons,  $P < 0.05$  for all treatment groups when compared to vehicle control (One-way ANOVA with Tukey's post hoc correction).

mum tolerated dose (MTD) studies conducted internally (data not shown). Consistent with the Lenvatinib effects described above, the combination of H3B-6527 and DC-101 showed tumor regressions in this Hep3B model pointing to tumor microenvironment as the driver of enhanced efficacy (TGI of 104.5% for the H3B-6527 and DC101 combination treatment group on day 18; **Figure 3D**). Taken together, these *in vitro* and *in vivo* data suggest that tumor microenvironment has a critical role in the Lenvatinib mediated enhancement of H3B-6527 efficacy.

*RNA-seq based MoA analysis shows anti-angiogenic effects as a major mediator of combination effect*

To further investigate the underlying mechanism of the enhanced combination effect of H3B-6527 and Lenvatinib, we conducted RNA-seq analysis of Hep3B cell line xenograft tumors following treatment of tumor bearing

mice with one dose of H3B-6527 or Lenvatinib as single agents or in combination. Principal component analysis and hierarchical clustering of differentially expressed genes (differentially expressed genes with adjusted  $p$  value  $< 0.05$ ) showed two largely separated groups in which vehicle and Lenvatinib samples are close to each other whereas the H3B-6527 and the combination samples show similar pattern (**Figure 4A** and **4B**), suggesting Lenvatinib at 10 mg/kg does not drastically alter transcriptional profiles of tumor cells [29]. We then performed pathway enrichment analysis of differentially expressed genes, which showed bile acid metabolism as the top upregulated pathway in H3B-6527 single-agent group, a well-known selective effect to the FGFR4 signaling pathway (**Figure 4C**) [30]. E2F targets and MYC targets scored as the top downregulated pathways; an effect that is common among many receptor tyrosine kinases including FGFR4

## Enhanced efficacy in HCC by combining FGFR4 and VEGFR inhibition

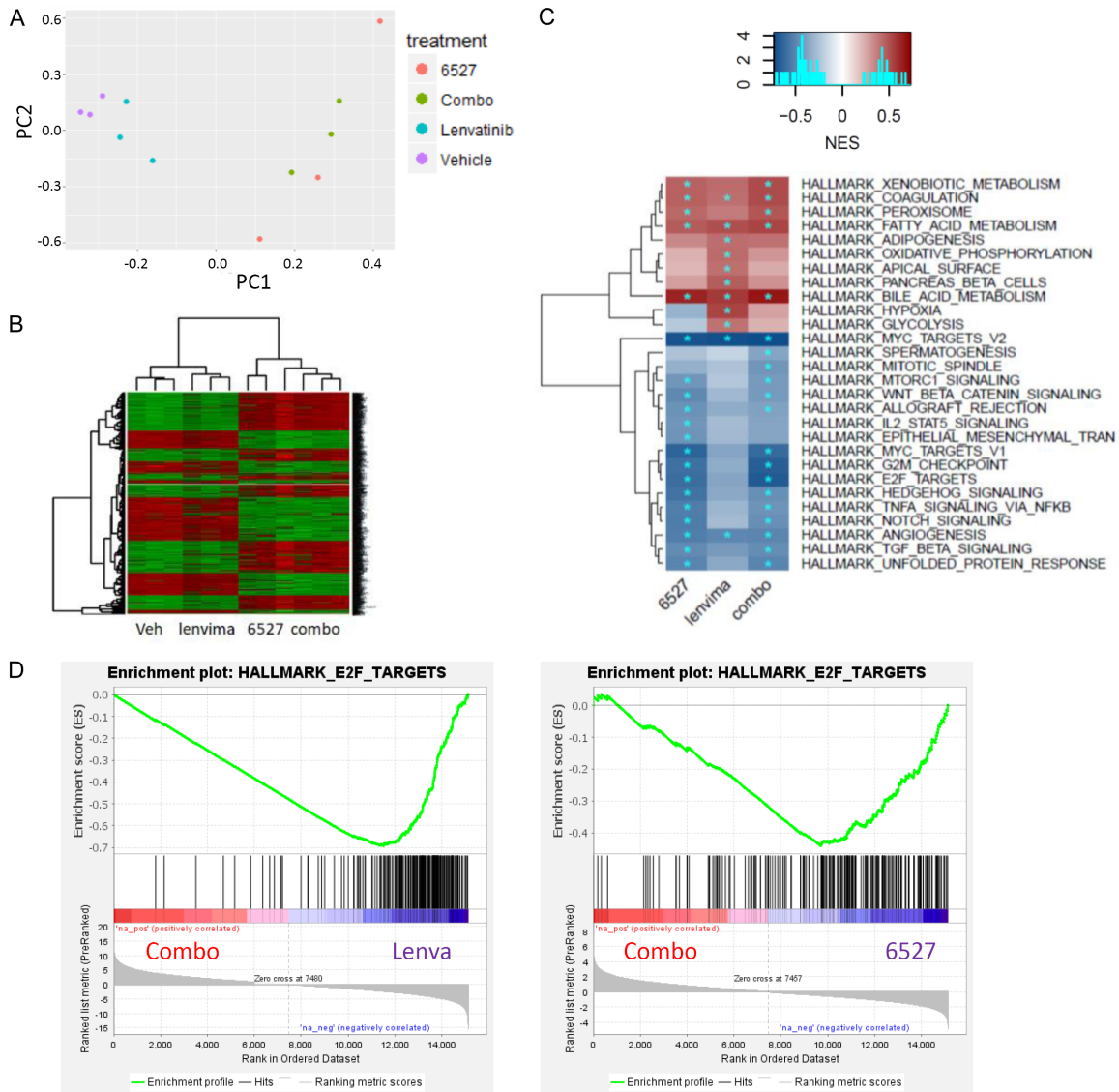


**Figure 4.** RNA-seq analysis following H3B-6527 and Lenvatinib as single agents or in combination in Hep3B *in vivo*. A. Principal component analysis of 1818 genes with largest variation. B. Hierarchical clustering analysis of top differentially expressed genes (differentially expressed genes with adjusted  $p$  value < 0.05). The samples are ordered by treatment. C. Functional annotation using GSEA analysis with Hallmark gene set collection by comparing treatment groups to vehicle. \* indicates functions with FDR  $q$ -value < 0.05. D. Enrichment plots of “Hallmark\_E2F\_TARGETS” gene set by comparing combination to single agents.

[31]. Combination of H3B-6527 and Lenvatinib showed significant upregulation of hypoxia and glycolysis pathways, consistent with anti-angiogenic effect resulting in lack of oxygen and nutrients in tumor microenvironment (**Figure 4C**). Moreover, the combination groups showed stronger effects on E2F targets as compared with the single agent groups, and explains the increased antitumor activity observed in efficacy experiments (**Figure 4D**). In summary, the RNAseq analysis provided direct mechanistic evidence for the combined anti-angiogenic and

anti-tumorigenic effects resulting in enhanced efficacy.

### *Lenvatinib enhances H3B-6527 antitumor effect in HCC PDX models*

Having established the combination effect of H3B-6527 and Lenvatinib in the Hep3B HCC model, we next sought to independently confirm these observations using additional *in vivo* models. To this end, we utilized seven FGF19 positive HCC patient derived tumor xenograft

## Enhanced efficacy in HCC by combining FGFR4 and VEGFR inhibition

**Table 1.** H3B-6527 plus Lenvatinib combination in a set of HCC PDX models. Response summary of PDX models *in vivo* efficacy data. Response = tumor stasis or regression

PDX Model number	FGF19 mRNA status	H3B-6527 single agent response	Lenvatinib single agent response	H3B-6527 + Lenvatinib combination response
		500 mg/kg QD	10 mg/kg QD	500 mg/kg QD + 10 mg/kg QD
HCC PDX 15	FGF19 (+)	Non responder	Non responder	Non responder
HCC PDX 28	FGF19 (+)	Non responder	Non responder	Responder
HCC PDX 8	FGF19 (+)	Non responder	Non responder	Non responder
HCC PDX 26	FGF19 (+)	Non responder	Non responder	Responder
HCC PDX 12	FGF19 (+)	Non responder	Non responder	Responder
HCC PDX 14	FGF19 (+)	Non responder	Responder	Responder
HCC PDX 11	FGF19 (+)	Responder	Non responder	Responder
		1/7 Responder	1/7 Responder	5/7 Responders

(PDX) models and tested the antitumor activity of H3B-6527 at 500 mg/kg, Lenvatinib at 10 mg/kg as single agents and in combination. The choice of the PDX model and dose level of H3B-6527 at 500 mg/kg was guided by the historical work [10]. Models in this combination study that showed tumor stasis or tumor regression following treatment are considered responders (see methods). Five out of seven models fell into the responder category following combination therapy whereas only one model can be classified as responder in the single agent groups (Table 1; Supplementary Figure 1 and Supplementary Table 1). Interestingly, three PDX models (HCC PDX 12, 26 and 28) did not respond to either single agent, but showed tumor stasis or regression in the combination group (Table 1). Taken together, these observations suggest that Lenvatinib in combination with H3B-6527 enhances H3B-6527 efficacy in a set of FGF19-overexpressing HCC PDX models.

### Discussion

Targeted therapies with patient enrichment strategies using biomarkers such as mutations and amplifications made inroads in many solid tumors, however, they are completely absent in HCC [32, 33]. The Discovery of FGF19 overexpression as a potential driver of ~30% HCC generated excitement due to the possibility of blocking the pathway through FGFR4 inhibitors. FGF19 overexpression is known to be driven by amplification of the FGF19 gene locus, 11q13, in about ~5% cases and the basis of overexpression in the rest of the subset is currently unknown [34]. To block FGFR4 and test the FGF19 hypothesis, we leveraged

the unique hinge cysteine in FGFR4 and developed a highly selective and covalent FGFR4 inhibitor, H3B-6527 [10]. Although recent clinical data of FGFR4 inhibitors, including H3B-6527 provided solid evidence for the single-agent activity, they also showed the limitation with regards to overall response rates and duration of response [12]. This prompted us to look for combination partners for H3B-6527.

We chose VEGFR pathway inhibition to combine with H3B-6527 for the following reasons. First, a hallmark of HCC is hypervascularity due to the critical role played by VEGFR pathways. Antiangiogenic agents such as Lenvatinib are the front-line treatment for the advanced-stage HCC patients. Second, the VEGFR and FGFR pathways are closely related, and they share common downstream signaling components. Both VEGFR and FGFR4 pathways exert important functions in promoting the cancer progression and metastasis through either direct tumor-autonomous or indirect non-autonomous effects [23, 35]. Third, in patients treated with anti-VEGFR therapies, FGFR4 pathway is reported to be responsible for the development of resistance [13], and vice versa, activation of VEGFR pathway is thought to confer resistance to anti-FGFR therapy. These lines of evidence provided the rationale for us to test the effect of combined inhibition of the FGFR and VEGFR pathways.

Our *in vivo* combination data in the Hep3B cell line xenograft model showed that Lenvatinib strongly enhanced the anti-tumor activity of H3B-6527. Lenvatinib is an approved agent for first-line HCC patients and its effects are largely mediated through VEGFRs. There are reports

## Enhanced efficacy in HCC by combining FGFR4 and VEGFR inhibition

that Lenvatinib, at high concentrations, can inhibit FGFR4 raising the possibility that the enhanced combination efficacy may have been due to deeper inhibition of FGFR4 in Hep3B [5, 25]. The lack of enhanced CYP7A1 upregulation, an FGFR4 downstream marker, provides evidence that the enhanced combination effect is not due to enhanced FGFR4 inhibition. On the question of whether Lenvatinib combination effects were mediated by cell-autonomous or cell non-autonomous pathways, the lack of a strong synergistic *in vitro* combination viability effect suggested that the efficacy observed *in vivo* is likely cell non-autonomous. In addition, strong *in vivo* combination efficacy with the mouse specific VEGFR2 antibody, DC101, which cannot cell-autonomously inhibit pathways in human xenografts, also support cell non-autonomous mode of action in Hep3B. DC-101 is the mouse specific surrogate Ramucirumab antibody that is suitable for selectively studying microenvironment in mouse xenograft settings [26, 27]. Among the VEGFRs, VEGFR2 is thought to be the critical player supported by the FDA approval of Ramucirumab in HCC. Hep3B cells do not express VEGFR2 and Ramucirumab treatment has no anti-tumor activity in Hep3B and minimal to no effect in enhancing H3B-6527 (data not shown). Mechanistic work through RNAseq analysis in Hep3B tumors revealed significant upregulation of hypoxia and glycolysis pathways, and down regulation of E2F targets, providing direct evidence for the combined anti-angiogenic and anti-tumorigenic effects resulting in enhanced efficacy. Lastly, our PDX panel work in FGF19 positive models provided solid evidence for the effectiveness and broader application of this combination.

Combination therapies are becoming a mainstay in cancer treatment to provide superior efficacy and to overcome tumor resistance by blocking escape routes. Previously we had reported the discovery of CDK4/6 inhibitor combination as a viable option to improve H3B-6527 efficacy and this combination is yet to be tested in the clinical setting [10]. CDK4/6 inhibitors are not approved in HCC and testing the FGFR4 inhibitor and CDK4/6 inhibitor combination may need lengthy development time due to the nature of combining two novel agents. In contrast, VEGFR combinations can be readily applied as many VEGFR inhibitors

and antibodies are already approved in HCC. Our preclinical work here showed that the combination of H3B-6527 and Lenvatinib resulted in enhanced efficacy through increased anti-angiogenic and anti-tumor activity providing the foundation to test this combination in clinical trials.

### Acknowledgements

The authors would like to thank the H3 coworkers for helpful discussions and advice.

### Disclosure of conflict of interest

None.

**Address correspondence to:** Anand Selvaraj and Xuesong Zhao, Department of Discovery, H3 Biomedicine, 300 Technology Square, Cambridge, MA 02139, USA. Tel: 617-252-5009; E-mail: anand\_selvaraj@h3biomedicine.com (AS); xuesong\_zhao@h3biomedicine.com (XSZ)

### References

- [1] Torrecilla S and Llovet JM. New molecular therapies for hepatocellular carcinoma. *Clin Res Hepatol Gastroenterol* 2015; 39 Suppl 1: S80-85.
- [2] Cheng AL, Shen YC and Zhu AX. Targeting fibroblast growth factor receptor signaling in hepatocellular carcinoma. *Oncology* 2011; 81: 372-380.
- [3] Draper A. A concise review of the changing landscape of hepatocellular carcinoma. *Am J Manag Care* 2020; 26: S211-S219.
- [4] Gordan JD, Kennedy EB, Abou-Alfa GK, Beg MS, Brower ST, Gade TP, Goff L, Gupta S, Guy J, Harris WP, Iyer R, Jaiyesimi I, Jhawer M, Karippot A, Kaseb AO, Kelley RK, Knox JJ, Kortmansky J, Leaf A, Remak WM, Shroff RT, Sohal DPS, Taddei TH, Venepalli NK, Wilson A, Zhu AX and Rose MG. Systemic therapy for advanced hepatocellular carcinoma: ASCO guideline. *J Clin Oncol* 2020; 38: 4317-4345.
- [5] Doycheva I and Thuluvath PJ. Systemic therapy for advanced hepatocellular carcinoma: an update of a rapidly evolving field. *J Clin Exp Hepatol* 2019; 9: 588-596.
- [6] Zucman-Rossi J, Villanueva A, Nault JC and Llovet JM. Genetic landscape and biomarkers of hepatocellular carcinoma. *Gastroenterology* 2015; 149: 1226-1239, e1224.
- [7] Pinyol R, Nault JC, Quetglas IM, Zucman-Rossi J and Llovet JM. Molecular profiling of liver tumors: classification and clinical translation for

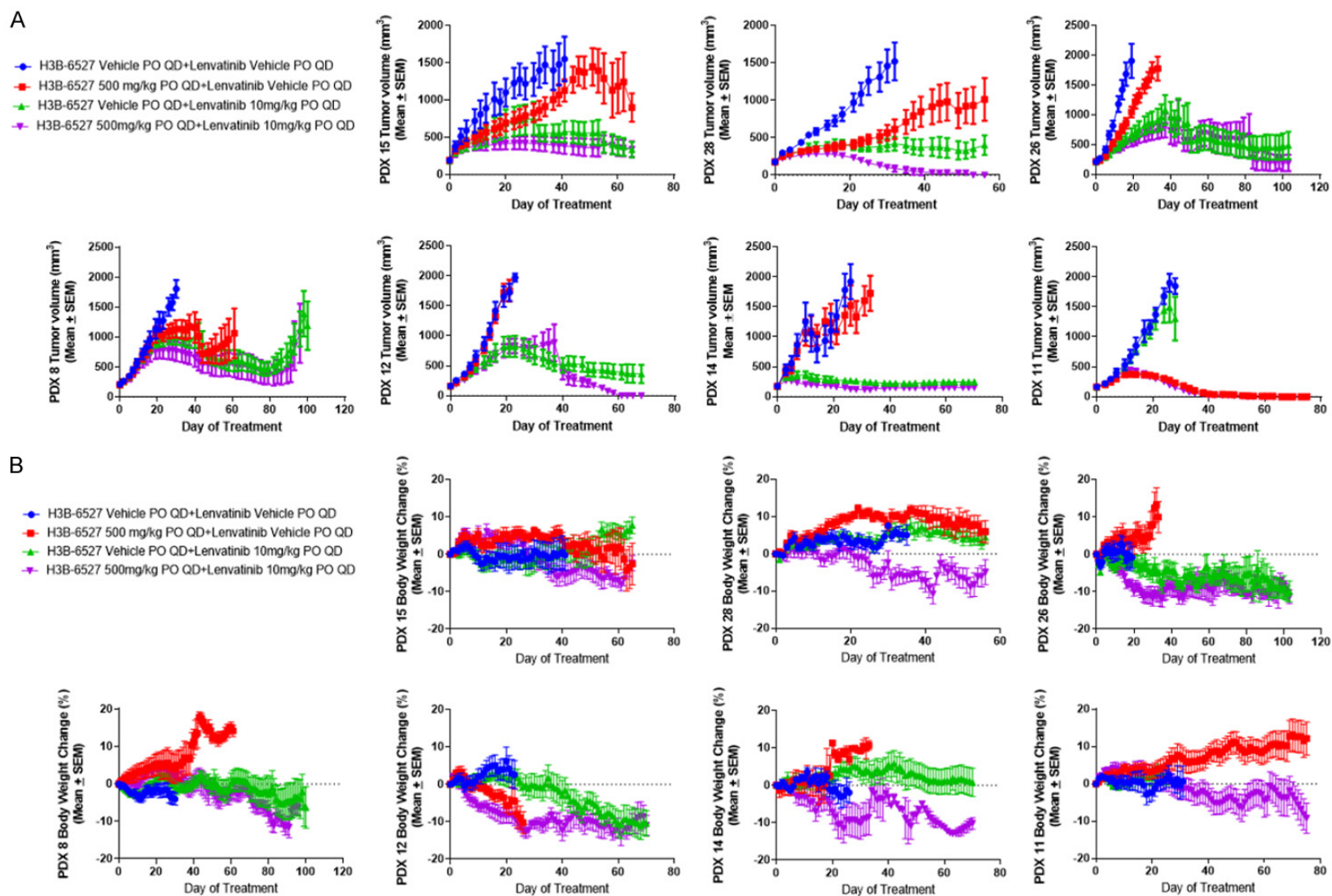
## Enhanced efficacy in HCC by combining FGFR4 and VEGFR inhibition

- decision making. *Semin Liver Dis* 2014; 34: 363-375.
- [8] Jones S. Mini-review: endocrine actions of fibroblast growth factor 19. *Mol Pharm* 2008; 5: 42-48.
- [9] French DM, Lin BC, Wang M, Adams C, Shek T, Hotzel K, Bolon B, Ferrando R, Blackmore C, Schroeder K, Rodriguez LA, Hristopoulos M, Venook R, Ashkenazi A and Desnoyers LR. Targeting FGFR4 inhibits hepatocellular carcinoma in preclinical mouse models. *PLoS One* 2012; 7: e36713.
- [10] Joshi JJ, Coffey H, Corcoran E, Tsai J, Huang CL, Ichikawa K, Prajapati S, Hao MH, Bailey S, Wu J, Rimkunas V, Karr C, Subramanian V, Kumar P, MacKenzie C, Hurley R, Satoh T, Yu K, Park E, Rioux N, Kim A, Lai WG, Yu L, Zhu P, Buonamici S, Larsen N, Fekkes P, Wang J, Warmuth M, Reynolds DJ, Smith PG and Selvaraj A. H3B-6527 is a potent and selective inhibitor of FGFR4 in FGF19-driven hepatocellular carcinoma. *Cancer Res* 2017; 77: 6999-7013.
- [11] Weiss A, Adler F, Buhles A, Stamm C, Fairhurst RA, Kiffe M, Sterker D, Centeleghe M, Wartmann M, Kinyamu-Akunda J, Schadt HS, Couttet P, Wolf A, Wang Y, Barzaghi-Rinaudo P, Murakami M, Kauffmann A, Knoepfel T, Buschmann N, Leblanc C, Mah R, Furet P, Blank J, Hofmann F, Sellers WR and Graus Porta D. FGF401, a first-in-class highly selective and potent FGFR4 inhibitor for the treatment of FGF19-driven hepatocellular cancer. *Mol Cancer Ther* 2019; 18: 2194-2206.
- [12] Kim RD, Sarker D, Meyer T, Yau T, Macarulla T, Park JW, Choo SP, Hollebecque A, Sung MW, Lim HY, Mazzaferro V, Trojan J, Zhu AX, Yoon JH, Sharma S, Lin ZZ, Chan SL, Faivre S, Feun LG, Yen CJ, Dufour JF, Palmer DH, Llovet JM, Manoojian M, Tugnait M, Stransky N, Hagel M, Kohl NE, Lengauer C, Sherwin CA, Schmidt-Kittler O, Hoeflich KP, Shi H, Wolf BB and Kang YK. First-in-human phase I study of fsgatinib (BLU-554) validates aberrant FGF19 signaling as a driver event in hepatocellular carcinoma. *Cancer Discov* 2019; 9: 1696-1707.
- [13] Gao L, Wang X, Tang Y, Huang S, Hu CA and Teng Y. FGF19/FGFR4 signaling contributes to the resistance of hepatocellular carcinoma to sorafenib. *J Exp Clin Cancer Res* 2017; 36: 8.
- [14] Dobin A, Davis CA, Schlesinger F, Drenkow J, Zaleski C, Jha S, Batut P, Chaisson M and Gingeras TR. STAR: ultrafast universal RNA-seq aligner. *Bioinformatics* 2013; 29: 15-21.
- [15] Bray NL, Pimentel H, Melsted P and Pachter L. Near-optimal probabilistic RNA-seq quantification. *Nat Biotechnol* 2016; 34: 525-527.
- [16] Robinson MD, McCarthy DJ and Smyth GK. edgeR: a Bioconductor package for differential expression analysis of digital gene expression data. *Bioinformatics* 2010; 26: 139-140.
- [17] Mootha VK, Lindgren CM, Eriksson KF, Subramanian A, Sihag S, Lehar J, Puigserver P, Carlsson E, Ridderstrale M, Laurila E, Houstis N, Daly MJ, Patterson N, Mesirov JP, Golub TR, Tamayo P, Spiegelman B, Lander ES, Hirschhorn JN, Altshuler D and Groop LC. PGC-1 $\alpha$ -responsive genes involved in oxidative phosphorylation are coordinately downregulated in human diabetes. *Nat Genet* 2003; 34: 267-273.
- [18] Subramanian A, Tamayo P, Mootha VK, Mukherjee S, Ebert BL, Gillette MA, Paulovich A, Pomeroy SL, Golub TR, Lander ES and Mesirov JP. Gene set enrichment analysis: a knowledge-based approach for interpreting genome-wide expression profiles. *Proc Natl Acad Sci U S A* 2005; 102: 15545-15550.
- [19] Shoemaker RH. The NCI60 human tumour cell line anticancer drug screen. *Nat Rev Cancer* 2006; 6: 813-823.
- [20] Zimmermann GR, Lehar J and Keith CT. Multi-target therapeutics: when the whole is greater than the sum of the parts. *Drug Discov Today* 2007; 12: 34-42.
- [21] Lehar J, Krueger AS, Avery W, Heilbut AM, Johansen LM, Price ER, Rickles RJ, Short GF 3rd, Staunton JE, Jin X, Lee MS, Zimmermann GR and Borisy AA. Synergistic drug combinations tend to improve therapeutically relevant selectivity. *Nat Biotechnol* 2009; 27: 659-666.
- [22] Xin H, Wang K, Hu G, Xie F, Ouyang K, Tang X, Wang M, Wen D, Zhu Y and Qin X. Establishment and characterization of 7 novel hepatocellular carcinoma cell lines from patient-derived tumor xenografts. *PLoS One* 2014; 9: e85308.
- [23] Morse MA, Sun W, Kim R, He AR, Abada PB, Mynderse M and Finn RS. The role of angiogenesis in hepatocellular carcinoma. *Clin Cancer Res* 2019; 25: 912-920.
- [24] Hagel M, Miduturu C, Sheets M, Rubin N, Weng W, Stransky N, Bifulco N, Kim JL, Hodous B, Brooijmans N, Shutes A, Winter C, Lengauer C, Kohl NE and Guzi T. First selective small molecule inhibitor of FGFR4 for the treatment of hepatocellular carcinomas with an activated FGFR4 signaling pathway. *Cancer Discov* 2015; 5: 424-437.
- [25] Yamamoto Y, Matsui J, Matsushima T, Obaishi H, Miyazaki K, Nakamura K, Tohyama O, Semba T, Yamaguchi A, Hoshi SS, Mimura F, Haneda T, Fukuda Y, Kamata JI, Takahashi K, Matsuura M, Wakabayashi T, Asada M, Nomoto KI, Watanabe T, Dezso Z, Yoshimatsu K, Funahashi Y and Tsuruoka A. Lenvatinib, an angiogenesis inhibitor targeting VEGFR/FGFR, shows broad antitumor activity in human tumor xenograft models associated with microvessel density and pericyte coverage. *Vasc Cell* 2014; 6: 18.

## Enhanced efficacy in HCC by combining FGFR4 and VEGFR inhibition

- [26] Witte L, Hicklin DJ, Zhu Z, Pytowski B, Kottanides H, Rockwell P and Bohlen P. Monoclonal antibodies targeting the VEGF receptor-2 (Flk1/KDR) as an anti-angiogenic therapeutic strategy. *Cancer Metastasis Rev* 1998; 17: 155-161.
- [27] Prewett M, Huber J, Li Y, Santiago A, O'Connor W, King K, Overholser J, Hooper A, Pytowski B, Witte L, Bohlen P and Hicklin DJ. Antivascular endothelial growth factor receptor (fetal liver kinase 1) monoclonal antibody inhibits tumor angiogenesis and growth of several mouse and human tumors. *Cancer Res* 1999; 59: 5209-5218.
- [28] Klement G, Baruchel S, Rak J, Man S, Clark K, Hicklin DJ, Bohlen P and Kerbel RS. Continuous low-dose therapy with vinblastine and VEGF receptor-2 antibody induces sustained tumor regression without overt toxicity. *J Clin Invest* 2000; 105: R15-24.
- [29] Cancer Genome Atlas Network. Comprehensive molecular portraits of human breast tumours. *Nature* 2012; 490: 61-70.
- [30] Yu C, Wang F, Kan M, Jin C, Jones RB, Weinstein M, Deng CX and McKeethan WL. Elevated cholesterol metabolism and bile acid synthesis in mice lacking membrane tyrosine kinase receptor FGFR4. *J Biol Chem* 2000; 275: 15482-15489.
- [31] Katz M, Amit I and Yarden Y. Regulation of MAPKs by growth factors and receptor tyrosine kinases. *Biochim Biophys Acta* 2007; 1773: 1161-1176.
- [32] Llovet JM and Hernandez-Gea V. Hepatocellular carcinoma: reasons for phase III failure and novel perspectives on trial design. *Clin Cancer Res* 2014; 20: 2072-2079.
- [33] Schulze K, Imbeaud S, Letouze E, Alexandrov LB, Calderaro J, Rebouissou S, Couchy G, Meiller C, Shinde J, Soysouvanh F, Calatayud AL, Pinyol R, Pelletier L, Balabaud C, Laurent A, Blanc JF, Mazzaferro V, Calvo F, Villanueva A, Nault JC, Bioulac-Sage P, Stratton MR, Llovet JM and Zucman-Rossi J. Exome sequencing of hepatocellular carcinomas identifies new mutational signatures and potential therapeutic targets. *Nat Genet* 2015; 47: 505-511.
- [34] Cancer Genome Atlas Research Network. Electronic address: wheeler@bcm.edu; Cancer Genome Atlas Research Network. Comprehensive and integrative genomic characterization of hepatocellular carcinoma. *Cell* 2017; 169: 1327-1341, e23.
- [35] Wang Y, Liu D, Zhang T and Xia L. FGF/FGFR signaling in hepatocellular carcinoma: from carcinogenesis to recent therapeutic intervention. *Cancers (Basel)* 2021; 13: 1360.

## Enhanced efficacy in HCC by combining FGFR4 and VEGFR inhibition



**Supplementary Figure 1.** H3B-6527 plus Lenvatinib combination effect in 7 HCC PDX models. Tumor volume (A) and body weight (B) measurements of 7 HCC PDX models at indicated days following oral dosing of H3B-6527 and Lenvatinib at indicated doses and schedule. QD, Once daily dose. PO, Per os (oral dosing). Data represent the mean  $\pm$  SEM (N = 8).

## Enhanced efficacy in HCC by combining FGFR4 and VEGFR inhibition

**Supplementary Table 1.** Summary of tumor growth inhibition in H3B-6527 plus Lenvatinib combination in 7 HCC PDX models (N = 8). TGI is calculated for each treatment versus vehicle control on the last day of vehicle treatment

PDx Model	Treatment	TGI (%)/Day
HCC PDX 15	H3B-6527	31.09/D41
	Lenvatinib	71.23/D41
	Combination	85.52/D41
HCC PDX 28	H3B-6527	67.35/D32
	Lenvatinib	82.04/D32
	Combination	106.61/D32
HCC PDX 8	H3B-6527	41.51/D30
	Lenvatinib	49.94/D30
	Combination	65.56/D30
HCC PDX 26	H3B-6527	50.81/D19
	Lenvatinib	72.97/D19
	Combination	80.77/D19
HCC PDX 12	H3B-6527	-1.80/D21
	Lenvatinib	57.72/D21
	Combination	57.02/D21
HCC PDX 14	H3B-6527	22.70/D26
	Lenvatinib	94.29/D26
	Combination	102.65/D26
HCC PDX 11	H3B-6527	96.04/D28
	Lenvatinib	31.94/D28
	Combination	100.34/D28